Hydrol. Earth Syst. Sci., 19, 3633–3651, 2015
www.hydrol-earth-syst-sci.net/19/3633/2015/
doi:10.5194/hess-19-3633-2015

Hydrology and Earth System Sciences
Open Access

Isolating the impacts of land use and climate change on streamflow

I. Chawla[1] **and P. P. Mujumdar**[1,2]

[1]Department of Civil Engineering, Indian Institute of Science, Bangalore, India
[2]Divecha Centre for Climate Change, Indian Institute of Science, Bangalore, India

Correspondence to: P. P. Mujumdar (pradeep@civil.iisc.ernet.in)

Received: 26 January 2015 – Published in Hydrol. Earth Syst. Sci. Discuss.: 20 February 2015
Revised: 3 August 2015 – Accepted: 10 August 2015 – Published: 24 August 2015

Abstract. Quantifying the isolated and integrated impacts of land use (LU) and climate change on streamflow is challenging as well as crucial to optimally manage water resources in river basins. This paper presents a simple hydrologic modeling-based approach to segregate the impacts of land use and climate change on the streamflow of a river basin. The upper Ganga basin (UGB) in India is selected as the case study to carry out the analysis. Streamflow in the river basin is modeled using a calibrated variable infiltration capacity (VIC) hydrologic model. The approach involves development of three scenarios to understand the influence of land use and climate on streamflow. The first scenario assesses the sensitivity of streamflow to land use changes under invariant climate. The second scenario determines the change in streamflow due to change in climate assuming constant land use. The third scenario estimates the combined effect of changing land use and climate over the streamflow of the basin. Based on the results obtained from the three scenarios, quantification of isolated impacts of land use and climate change on streamflow is addressed. Future projections of climate are obtained from dynamically downscaled simulations of six general circulation models (GCMs) available from the Coordinated Regional Downscaling Experiment (CORDEX) project. Uncertainties associated with the GCMs and emission scenarios are quantified in the analysis. Results for the case study indicate that streamflow is highly sensitive to change in urban areas and moderately sensitive to change in cropland areas. However, variations in streamflow generally reproduce the variations in precipitation. The combined effect of land use and climate on streamflow is observed to be more pronounced compared to their individual impacts in the basin. It is observed from the isolated effects of land use and climate change that climate has a more dominant impact on streamflow in the region. The approach proposed in this paper is applicable to any river basin to isolate the impacts of land use change and climate change on the streamflow.

1 Introduction

Land use (LU) and climate are the drivers of hydrologic processes in a river basin (Vörösmarty et al., 2000; Nijssen et al., 2001; Oki and Kanae, 2006; Wada et al., 2011). Change in LU is observed to influence the hydrological cycle and the availability of water resources by altering interception, infiltration rate, albedo and evapotranspiration (ET) (Rose and Peters, 2001; Scanlon et al., 2007; Rientjes et al., 2011). Climate in contrast affects the basic components of hydrologic cycle such as precipitation, soil moisture, evaporation and atmospheric water content (Gleick, 1986; Wang et al., 2008). Therefore, understanding the hydrologic response of a river basin to changes in LU and climate forms a critical step towards water resources planning and management (Vörösmarty et al., 2000). Moreover, with increase in scarcity of water resources, hydrologic impacts of LU and climate change have drawn significant attention from the hydrologic community (Scanlon et al., 2007). In this regard, several studies have been carried out that focus on understanding exclusive impacts of either of the two drivers (Hamlet and Lettenmaier, 1999; Christensen and Lettenmaier, 2007; Beyene et al., 2010; Wagner et al., 2013; Islam et al., 2014). However, optimum management of water resources in a river basin needs an in-depth understanding of the isolated and integrated effects of LU and climate on streamflow. Due to complex response of streamflow to combined effects of LU and

climate change (Fu et al., 2007; Guo et al., 2008), very few studies have been carried out on this aspect (Mango et al., 2011; Guo et al., 2008; Cuo et al., 2013; Wang et al., 2013). Segregating the individual contribution of LU and climate to streamflow has recently become the focus of scientific work (Wang and Hejazi, 2011; Wang et al., 2013; Renner et al., 2012, 2014).

Methods used to assess the impacts of LU and climate on streamflow can be broadly classified into four categories: (i) experimental paired catchment approach, (ii) statistical techniques such as Mann–Kendall test, (iii) empirical or conceptual models and (iv) distributed physically based hydrologic models. Among these techniques, the paired catchment approach is most difficult but often considered as the best approach for smaller catchments. However, applicability of the paired catchment approach over large catchments may not be possible (Lørup et al., 1998) since it requires years of continuous monitoring to gather sufficient data for the analysis. Statistical trend detection tests have been proved to be very useful in qualitatively determining the presence of a significant trend in the time series along with direction and rate of change (Zhang et al., 2008; Li et al., 2009). But these techniques cannot be used for quantifying the change and attributing it to a particular cause due to a lack of a physical mechanism (Li et al., 2009). Empirical or conceptual models are simple hydrologic models that require only a few parameters to simulate a catchment. However, a major drawback with these models is that the parameters may not be directly related to the physical conditions of the catchment, and thus may lack the ability to correctly represent a catchment. Therefore, one is left with the option of using distributed physically based hydrologic models, which are by far the most appealing tools to carry out impact assessment studies (Ott and Uhlenbrook, 2004; Mango et al., 2011; Wang et al., 2012). These models operate within a distributed framework to take physical and meteorological conditions of the basin into account (Refsgaard and Knudsen, 1996). Physically distributed models include both fully distributed and semi-distributed models. Owing to their extensive parameterization, fully distributed models are difficult to employ at a large catchment scale which make comparatively less data-intensive semi-distributed models a practical alternative. This paper presents a simple hydrologic modeling-based approach to isolate the impacts of land use and climate on streamflow. For this purpose, a physically based macroscale variable infiltration capacity (VIC) hydrologic model (Liang et al., 1994) has been employed for the analysis.

In the present paper, Ganga River basin in India is selected as the case study to perform the analysis. Few studies have been reported in literature (Nijssen et al., 2001; Arora and Boer, 2001; Nohara et al., 2006) wherein Ganga basin is studied alongside other major river basins of the world (to assess the effect of changing climate on flow regime); however, there is a dearth of studies that comprehensively examine the effects of LU and climate change on streamflow exclusively in this basin. Originating from the Himalayas, the Ganga River traverses a stretch of 2525 km covering a catchment area of around 800 000 km^2, which is approximately 26 % of India's entire land mass making it the largest river basin in India. During its course, the Ganga River flows through some of the major states of India harboring about 44 % of the country's population (http://censusindia.gov.in/). Due to presence of alluvium, the basin is very fertile and forms close to 30 % of India's cultivable area (http://eands.dacnet.nic.in/LUS2001-11.htm). Thus, there is a clear consensus that the river is of great social and economic importance to India. In this study, the area under investigation is the upstream reaches of the Ganga basin encompassing the river's source (Fig. 1). This region is referred as the upper Ganga basin (UGB) in the paper. LU analysis carried out by Tsarouchi et al. (2014) on the UGB suggests that, between 1984 and 2010 the basin experienced an increase in urban and cropland area and decrease in barren land area.

In order to obtain the isolated impacts of LU and climate change on streamflow, the following objectives are addressed in the current work: (i) assessing sensitivity of the streamflow to changes in different LU categories, (ii) examining impacts of climate change on the streamflow and (iii) analyzing integrated impacts of LU and climate change on the streamflow. The three objectives are translated into three scenarios wherein the first two scenarios quantify the independent effects of LU and climate on streamflow under their invariant counterparts; i.e., climate and LU respectively are kept constant. The third scenario deals with concurrent changes in LU and climate. Results from the three scenarios are further used to segregate the hydrologic impacts of LU and climate change. The aforementioned objectives are investigated over the UGB as a case study by employing a calibrated and validated VIC model to simulate streamflows. To assess the impact of future climate on streamflow in the basin, dynamically downscaled climate simulations for six general circulation models (GCMs) obtained from the Coordinated Regional Downscaling Experiment (CORDEX) project are used. Climate change related analyses are carried out under the uncertainty framework to address two issues: (1) climate model-based uncertainties and (2) emission-scenario-based uncertainties.

2 Data and methods

2.1 Study area

The UGB (25°30′ N–31°30′ N, 77°30′ E–80° E) (Fig. 1) drains a catchment area of 95 593 km^2. While most of the Ganga basin comprises of agricultural areas with reasonably flat terrain, this region (UGB) is the only part of the Ganga basin that is characterized by a wide variation in topography with elevations ranging from 21 to 7796 m (Fig. 1), thus making it an interesting case study for investigation. In ad-

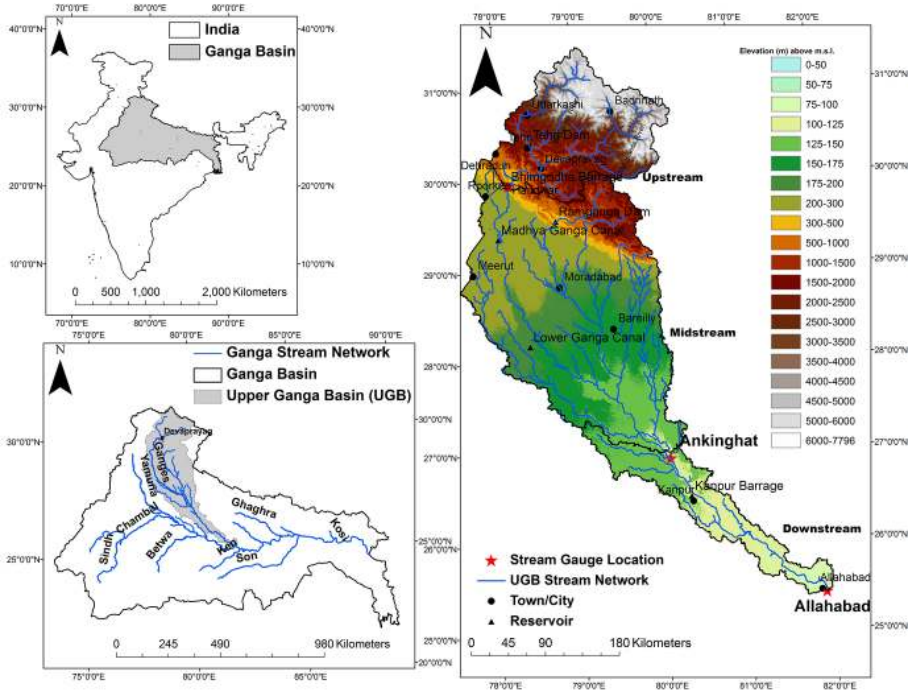

Figure 1. Location map and details of the UGB.

dition, since the Ganga River originates in this region, any change in hydrologic response due to LU and/or climate is likely to affect the entire flow regime downstream. Thus, this region is critical for assessing the impacts of LU and climate change on the streamflow of the basin. In the backdrop of a recent flood event in July 2013 in the UGB, which has been attributed to climate change (Singh et al., 2014), isolating the hydrologic impacts of changing LU and climate in this basin has become much more important.

In this study, the UGB is divided into three regions, upstream, midstream and downstream (Fig. 1), based on altitude, topography and land use characteristics. The upstream region is highly mountainous, characterized by glaciers and dense forests, with elevations from 297 to 7796 m. From upstream to midstream regions, there is a transition from hills to plains. The midstream region is dominated by forests and croplands with elevations ranging from 75 to 3079 m. The downstream region is mostly covered by croplands with consistent elevations of around 100 m. In addition to the varying land use characteristics, these three regions have different climatology as well. From 1971 to 2005, upstream, midstream and downstream regions recorded an average annual precipitation of 1294, 1009 and 826 mm, respectively. Most of the precipitation was concentrated during the monsoon months from June to September (JJAS). Average annual temperatures across the three regions during the same period were 20, 23 and 26 °C, respectively. Due to significant variation in the characteristics of these regions, they are modeled separately in the paper. Details of data required to drive the hydrologic model are presented in the following section.

2.2 Input data for the hydrologic model

The current study employs physically based VIC hydrologic model for the analysis. The VIC model is a semi-distributed soil–vegetation–atmosphere transfer model that solves coupled water and energy balance equations in a grid to calculate different hydrologic components (Liang et al., 1994). Within a grid the VIC model considers sub-grid heterogeneity by dividing each grid cell into a number of tiles which in turn depend on different land use types present in the grid. Each tile generates different responses to precipitation in the form of infiltration, soil moisture storage, runoff and evaporation, owing to a difference in land surface properties. When VIC concludes the computation of energy and water balance calculations for each grid within the watershed, a streamflow routing model developed by Lohmann et al. (1998) is activated, which transports the surface runoff generated within a grid along with the baseflow to the outlet of the grid cell which is further routed through the river channel to the watershed outlet.

Hydrologic models in general require topographic, soil, hydro-meteorological and LU data which can be procured from various sources. In the present work, topographic information is obtained from the ASTER (Advanced Spaceborne Thermal Emission and Reflection Radiometer) DEM (digital elevation model) available at 30 m spatial resolution. The digital soil map for the region is procured from

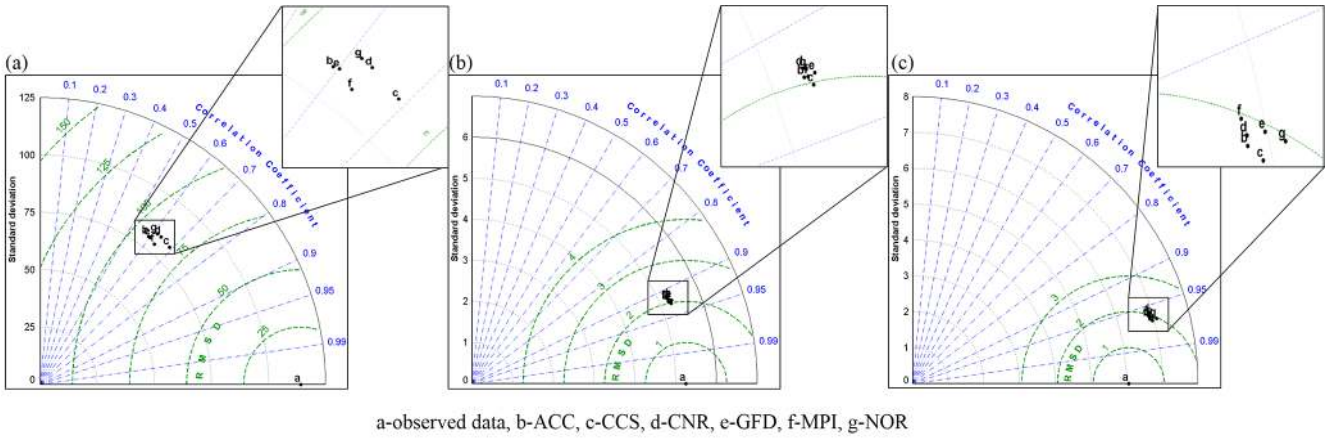

Figure 2. Taylor diagram for **(a)** rainfall (mm), **(b)** T_{max} (°C) and **(c)** T_{min} (°C) for the upstream region.

the National Bureau of Soil Survey and Land Use Planning, India, at a scale of 1 : 250 000. Meteorological data (rainfall, maximum temperature, minimum temperature and wind speed) for the period 1971–2005 at daily timescales are procured from two sources: the Indian Meteorological Department (IMD) (Rajeevan et al., 2006) and Princeton University (PU) (Sheffield et al., 2006). Meteorological data from both sources are brought to a common grid resolution of 0.5° that also serves as the resolution for executing the VIC hydrologic model. Observed streamflow data (Q_{obs}) for two locations, Bhimgodha (1987–2011) and Ankinghat (1977–2009), are obtained (at monthly scale) from the Uttar Pradesh Irrigation Department and Central Water Commission (CWC). Between the Bhimgodha and Ankinghat stations, there are diversions such as the Upper Ganga canal (UGC), Madhya Ganga canal (MGC) and Lower Ganga canal (LGC) (Fig. 1) that divert water from the main Ganga River. Therefore, along with Q_{obs}, data corresponding to various diversion channels are also procured from CWC and added to the observed (regulated) flow thereby converting the observed streamflow to a naturalized flow (Q_{n-obs}). The flow data thus obtained (Q_{n-obs}) are used for model calibration and validation.

For LU data, landsat imageries for the years 1973, 1980, 2000 and 2011 are selected and then classified to determine the LU change in the basin over 4 decades. A field study is carried out to collect the training sites for image classification. The accuracy of classified images is obtained to be 89, 83, 88 and 79% for 1973, 1980, 2000 and 2011 images, respectively, which is seen to be generally good. Thus, the classified images can be used as LU maps of the UGB for the corresponding time periods. Results of classification and change in LU are presented in Sect. 3.1.

To carry out hydrologic impact studies related to climate change, one needs data on future climate variables, such as rainfall (P), temperature (T) and wind speed (W), which in the current study are procured from the CORDEX South Asia group (http://cccr.tropmet.res.in/cordex/index.jsp) at a daily scale for six Coupled Model Intercomparison Project 5 (CMIP5) GCM simulations (Table 1). Each model has a time series for all the requisite variables corresponding to twentieth century climate (historic run) and future climate using Representative Concentration Pathway (RCP4.5 and RCP8.5) emission scenarios. All the GCM outputs are brought to a consistent resolution of 0.5°.

It is now well known that large-scale pattern of climate variables simulated by GCMs may be realistic, but when downscaled to a regional level, they may exhibit significant bias compared to the observed data (Maurer and Hidalgo, 2008; Ghosh and Mujumdar, 2009). This can have a significant effect on hydrological impact studies which necessitates the need of performing bias correction on the climate variables obtained. In the current work, climate variables obtained from the GCMs are bias corrected with IMD gridded data (which are considered as observed data) at a daily scale using the technique developed by Wood et al. (2002). A distribution function is fit to the observed daily data and individual GCM data. $F_{GCM}(x)$ of a GCM simulation is identified for a given x and the corresponding observed value x' is obtained from the observed cumulative distribution function (CDF), $F_{obs}(x')$ such that $F_{obs}(x') = F_{GCM}(x)$. GCM value x is then replaced with the observed value x' on the CDF of GCM.

Statistics of GCM simulated (post-bias correction) and observed climate variables for the upstream region are presented in a Taylor diagram (Fig. 2). It can be observed that all the models are clustered together, which could be due to the fact that all the GCM outputs are from the same modeling center, and the clusters in the case of T_{max} (maximum temperature) and T_{min} (minimum temperature) (Fig. 2b and c, respectively) are closer to the observed data (represented by point "a") that reflect a better quality of GCM outputs for T. In the case of P (Fig. 2a), it is observed that the models' cluster is slightly far from point "a"; nevertheless, a reason-

Table 1. GCMs from the CORDEX project used in the present study.

Modeling center – experiment name	Driving GCM (abbreviation)	Institution
Commonwealth Scientific and Industrial Research Organization, (CSIRO) Australia – CCAM	ACCESS1.0 (ACC)	CSIRO
	CNRM-CM5 (CNR)	Centre National de Recherches Météorologiques
	CCSM4 (CCS)	National Center for Atmospheric Research
	GFDL-CM3 (GFD)	Geophysical Fluid Dynamics Laboratory
	MPI-ESM-LR (MPI)	Max Planck Institute for Meteorology (MPI-M)
	NorESM1-M (NOR)	Norwegian Climate Centre

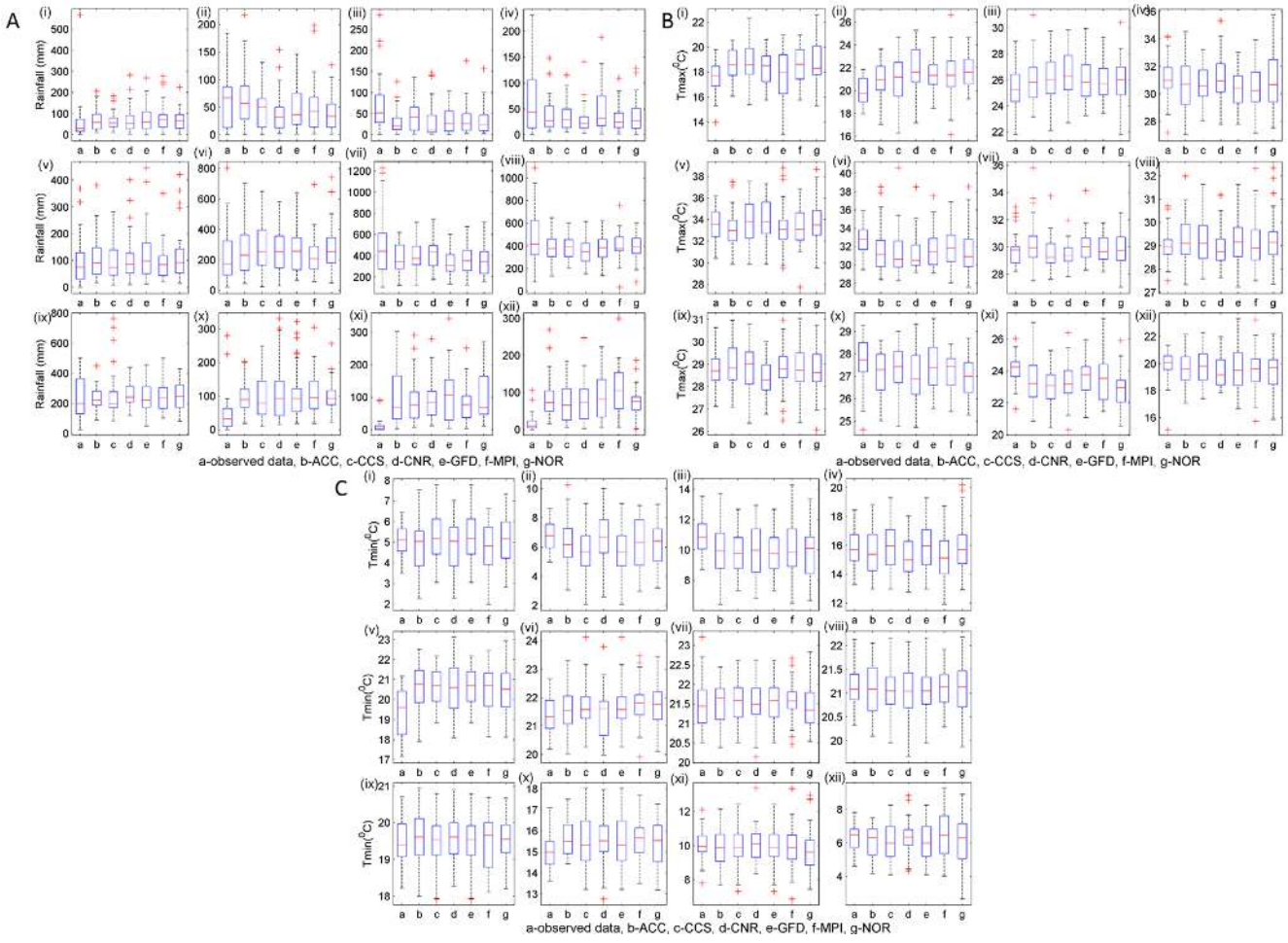

Figure 3. GCMs climatology compared with observed climatology for monthly **(a)** rainfall, **(b)** maximum temperature and **(c)** minimum temperature from 1971 to 2005 (represented from January to December as i–xii).

ably good correlation of 0.6–0.7 exists between GCM P and observed P. Similar inferences are drawn from the analyses over midstream and downstream regions.

In addition to the correlation coefficient, climatology of variables for different GCMs is compared with the climatology of the observed variable from 1971 to 2005 at a monthly scale. These results are presented in Fig. 3 for one of the grid cells within the UGB. The observed and GCM climatology at a monthly scale for the time period 1971–2005 is represented following Wood et al. (2002). It can be seen in Fig. 3 that the GCMs successfully reproduce the mean and variance of the rainfall climatology for most of the months. How-

Table 2. Structure of the VIC model obtained for upstream and midstream regions along with the performance measures during calibration and validation phase.

Region	No. of candidate models	Value of optimum set of parameters	Calibration				Validation			
			R^2	E_{NRMSE}	E_{NSE}	β	R^2	E_{NRMSE}	E_{NSE}	β
Upstream	47	$B = 0.13$, $D_s = 0.0005$, $W_s = 0.76$	0.77	0.23	0.77	−0.02	0.83	0.29	0.79	−0.18
Midstream	80	$B = 0.044$, $D_s = 0.0004$, $W_s = 0.62$	0.88	0.14	0.86	0.12	0.71	0.47	0.53	−0.04

ever, for the post-monsoon period (i.e., October, November and December), GCMs overestimate rainfall compared to the observed rainfall. For T_{max} and T_{min} (Fig. 3b and c, respectively), GCMs could successfully reproduce the observed climatology across all the months. Other grids within the UGB were found to demonstrate a similar pattern for both rainfall and temperature. Based on this analysis, downscaled variables are considered to reasonably represent the climate of the region and are further used to drive the VIC model.

In addition to the meteorological data and LU information, VIC requires explicit information about the vegetation type in the study region. In the study area, it is observed from the agricultural statistics (http://mospi.nic.in/MospiNew/site/India_Statistics.aspx) that wheat is grown in abundance during the rabi season (October–March), while rice and millet are grown during the kharif season (July–October). Furthermore, sugarcane is also grown in the upstream region of the UGB. Therefore, vegetation parameters corresponding to these four crops are provided as input to the relevant grid cells within the UGB.

2.3 VIC hydrologic model: calibration and validation

For the model calibration in the present work, three parameters as suggested by Lohmann et al. (1998) are calibrated to obtain an optimum combination such that the error between observed and simulated streamflow is at a minimum. The three parameters considered are (i) B – the variable infiltration curve parameter; (ii) D_s – the fraction of maximum velocity of baseflow where nonlinear baseflow begins; and (iii) W_s – the fraction of maximum soil moisture where nonlinear baseflow occurs. According to Liang et al. (1994), the parameter B has the largest effect on runoff hydrograph, and the D_s and W_s parameters are critical in influencing the baseflow. Calibration of these parameters is necessary since their values vary with catchments. Moreover, these are the only three parameters which are unknown in the present study. All the other parameters (http://www.hydro.washington.edu/Lettenmaier/Models/VIC/Documentation/SoilParam.shtml) are obtained from the soil map used in this study.

The VIC model is established independently for upstream, midstream and downstream regions but model calibration is only possible for upstream and midstream regions since Q_{obs} is not available for the downstream region. To address this issue, utilizing the facts that the downstream region has soil type similar to that of the midstream region (loam and sandy loam) and the three parameters are essentially influenced by soil, it is assumed that the calibrated parameters obtained for midstream will suffice for the downstream region.

To perform model calibration, initially the sensitivity of the simulated discharge to each of the three parameters is tested and their rough estimate of range for both upstream and midstream regions are obtained. Within this range, several candidate models for upstream and midstream regions are created based on several plausible combinations of these three parameters. The VIC model is executed for all the combinations and the one that has the maximum predictive power in terms of coefficient of determination (R^2), normalized root mean square error (E_{NRMSE}), Nash–Sutcliffe efficiency (E_{NSE}) and bias (β) for monthly series of simulated streamflow (Q_{sim}) during the calibration period is considered. Here, a negative value of β indicates that the model overestimates the simulated data and vice versa. It is to be noted that, though the VIC model is executed at a daily scale, daily Q_{sim} values are aggregated to monthly values to carry out comparison between Q_{sim} and Q_{n-obs} since Q_{n-obs} is only available at a monthly scale.

For the current work, the periods of 1987–1999 and 1977–1995 in upstream and midstream regions, respectively, are considered for calibration. Figure 4 provides the plots of corresponding observed and calibrated VIC simulated monthly streamflow series for the two regions. It can be observed from Fig. 4 that simulations during the calibration period captured the observed pattern and magnitude of hydrograph very well. In particular, rising and recession limbs of hydrographs are simulated accurately for both the regions. Shortcomings in the VIC simulations for both the regions include a mismatch of peak flows, which could be due to errors in modeling ex-

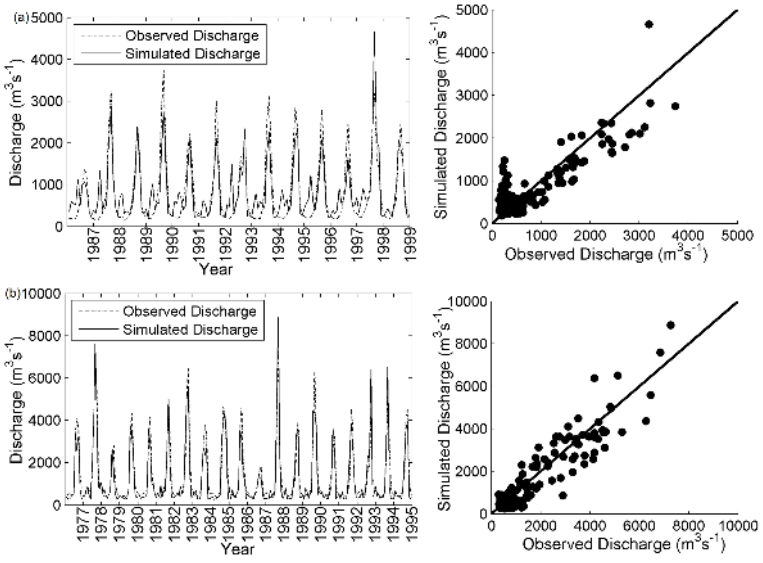

Figure 4. Calibration results of **(a)** upstream and **(b)** midstream regions.

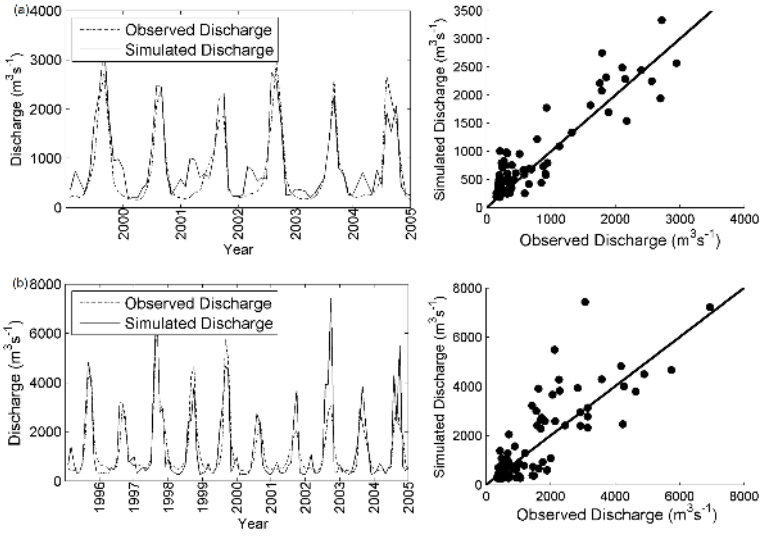

Figure 5. Validation results of **(a)** upstream and **(b)** midstream regions.

treme precipitation by the model. Since we are not dealing with extremes in the present case study, this error is not of much concern. In addition, it may also be observed that at the end of each recession limb, there is a sharp drop, which is below the level of $Q_{n-\mathrm{obs}}$. It could be due to inconsideration of baseflow contribution from the groundwater in Q_{sim} that needs to be included in Indian watersheds, wherein groundwater serves as major contributor to the streamflow in the form of baseflow during the months of November to March. Also, in the upstream region, some infrequent peaks are simulated by the model during low-flow periods which can be attributed to the overestimation of snowmelt runoff by the snow module (which is kept active) in the region. Pre- and post-monsoon rainfall events could also result in this kind of behavior.

The calibrated models are validated from 2000 to 2005 and from 1996 to 2005 for upstream and midstream regions, respectively (presented in Fig. 5). The streamflow pattern and magnitude of runoff are well simulated during the validation. Table 2 presents optimum set of parameters for the two regions along with their performance measures during calibration and validation. Based on the performance measures, it is seen that the model is able to predict $Q_{n-\mathrm{obs}}$ reasonably well. A slight negative β (which is evident from scatter plot of Fig. 4a) is observed for the upstream region, which could be due to overestimation of low-flow values. A positive β for the midstream region could be due to a lack of groundwater

contribution to Q_{sim}. The rigorously calibrated and validated VIC model is used to simulate the streamflow under different scenarios considered in the present study.

2.4 GCM and emission scenario uncertainty

Despite strong correlation between the model simulated and observed climate variables (Fig. 2), it is noticed that the magnitude of uncertainty across different models is quite large with respect to observed P and T at an annual scale. These uncertainties may get manifested in the hydrologic response (Arnell, 2011) when the future projections are used to drive the VIC hydrologic model for impact assessment. As a result it is essential to quantify the uncertainties associated with both climate data and streamflow generated from the VIC model, which, in the present work, is carried out over six GCMs and two emission scenarios. The uncertainty is quantified with a root mean square difference (σ) metric given by Eq. (1) (Giorgi and Mearns, 2002; Ekström et al., 2007).

$$\sigma = \left[\frac{1}{n}\sum_{i=1}^{n}\left(\Delta X_i - \overline{\Delta X}\right)^2\right]^{\frac{1}{2}}, \quad (1)$$

where n is the number of GCMs for a given RCP, X the variable under study, ΔX_i the change in the ith model mean value from the mean of the baseline period of the variable X and $\overline{\Delta X}$ the ensemble average of change in the mean given by Eq. (2):

$$\overline{\Delta X} = \frac{1}{n}\sum_{i=1}^{n}\Delta X_i. \quad (2)$$

In the present work, $\overline{\Delta X}$ is considered as an estimate of the effect of climate change. σ quantifies the average deviation of change in individual model mean from the ensemble average of change in mean. The higher the σ, the greater is the uncertainty associated with the $\overline{\Delta X}$ and consequently less reliable are the results. Further, the ensemble mean of models is statistically analyzed with the baseline period mean to test for equality of means using two sampled t test. The results of the t test are interpreted in terms of confidence levels for the change in future projections with respect to a baseline period.

In order to infer the confidence level in terms of climatology, the classification considered by Maurer (2007) is used whereby a confidence level (i) > 90 % indicates a highly significant change, (ii) 67–90 % indicates moderately significant change and (iii) < 67 % indicates insignificant change. Furthermore, the same test is used to estimate the confidence level with which it can be claimed that the two emission scenarios give statistically different ensemble means. Figure 6 presents the overview of the work.

Table 3. LU analysis of UGB for years 1973, 1980, 2000 and 2011.

Category	Area (% of total area of 95 593 km^2)			
	1973	1980	2000	2011
Snow	9.5	10.4	6.5	5.5
Dense forest	14.5	12.8	11.4	14.8
Scrub forest	23.6	14.8	13.9	9.0
Cropland	45.1	53.2	64.3	66.2
Barren land	5.0	6.4	0.6	0.2
Urban area	1.5	1.6	2.3	3.2
Water	0.7	0.9	1.0	1.1

3 Results and discussion

Section 3.1 and 3.2 provide analysis pertaining to the quantification of changes observed in LU and climate. In Sect. 3.3, these results are used to quantify streamflow variations within the uncertainty framework.

3.1 Analysis of land use

Classification of landsat imageries resulted in LU maps for the UGB that are presented in Fig. 7. It can be observed that the UGB exhibits wide variations in LU wherein upstream parts are snow covered and downstream parts are cropland. The dominant LU type in the UGB is cropland that covers about 56 % of the entire basin (45, 53, 64 and 66 % for 1973, 1980, 2000 and 2011, respectively). Upon visual examination of figures, it is evident that from 1973 to 2011, area under forest in the upstream region has diminished significantly. The percentage of total basin area under different LU categories in the UGB for different time periods is provided in Table 3.

It should be noted that for the present study, detailed snow cover mapping is not performed. Thus, the percentage area observed under the snow category in Table 3 should not be considered as a trend in the snow cover of the region. The urban category is observed to occupy far less area in the basin (< 5 %) across all the time periods. For dense forest area, a decline was observed from 1973 to 2000 followed by an increase. The reason could be attributed to better forest management strategies that are introduced in the region after creation of the Uttarakhand state in November 2000. It is observed that there is a slight increase in the surface area of water that could be attributed to the development of structures such as the Ramganga reservoir (Fig. 1) after 1973. Results reflect that there has been a massive increase in the area under cultivation in the basin. The dynamics of LU is heavily supported by a rapid increase in the population of the region (120 % increase between 2001 and 2011 as per census of India; http://censusindia.gov.in/). The impact of changes in LU over streamflow is assessed in Sect. 3.3.1. The following section provides analysis of climate change in the UGB.

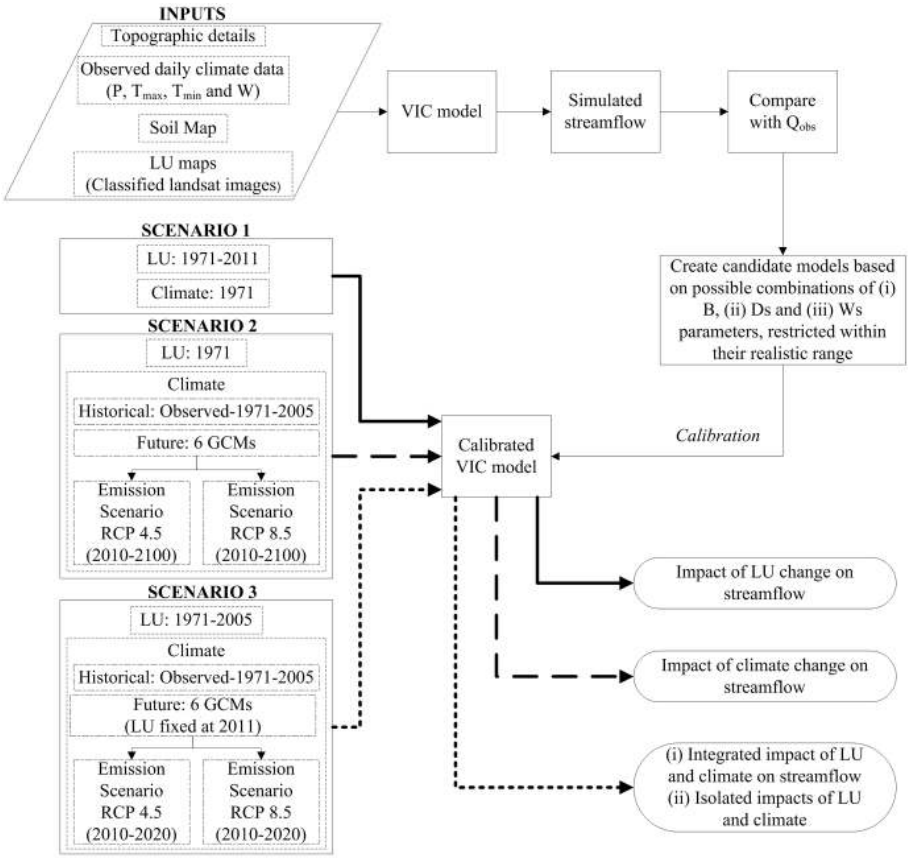

Figure 6. Overview of the work.

3.2 Analysis of climate variables

Observed rainfall obtained from IMD and projections of rainfall (P) obtained from GCMs are examined for long-term trends using Mann–Kendall test (Mann 1945; Kendall, 1938). It is noticed that observed P did not show any trend during the period 1971–2005 for upstream, midstream and downstream regions. However, projections of P exhibit a monotonic increase at an annual scale during the period 2010–2099 for all the regions with large inter-annual variability. In order to determine the change in the climatology of the three regions, outputs from GCMs for future time periods are aggregated into five time slices: T1 (2010–2020), T2 (2021–2040), T3 (2041–2060), T4 (2061–2080) and T5 (2081–2100). Further on, comparisons are made between the means of the future time slices and the baseline period (1971–2005). Figure 8 (top panel) shows average change in annual P over all GCMs ("ensemble mean change") in future time slices from the baseline period which is calculated using Eq. (2). Associated with the ensemble mean change is uncertainty, obtained using Eq. (1), which is represented by error bars in the figure. Uncertainty limits reflect the average deviation of change in the mean of individual GCMs from the ensemble mean.

T2 in case of RCP4.5 emission scenario is observed to exhibit maximum change for all the three regions along with high uncertainties. High confidence level associated with T2 imply probable impacts in hydrologic response associated with this time slice. The RCP8.5 emission scenario, for most of the time slices, exhibits moderately significant change which may result in less probable impacts.

Upon assessing the monthly variability in P, it is observed that it may decline significantly during monsoon months, whereas there might be an increase during winter months (October, November, December, January) across the three regions. This may result in shift in seasonal pattern of P in the region. Furthermore, if analyzed longitudinally from upstream to downstream it is noticed that the variation in P in the downstream region is much more severe.

On analyzing the trend in observed and projected annual mean T_{max} and T_{min}, it is noticed that observed annual mean T_{max} did not show any trend during 1971–2005, while observed annual mean T_{min} depicted an increasing trend during the same period. However, projected annual mean T_{max} and T_{min} are observed to show an increasing trend for future scenarios. Upon assessing the monthly variability, mean T_{max} and T_{min} are observed to increase significantly during winter months and they may decline during April to September

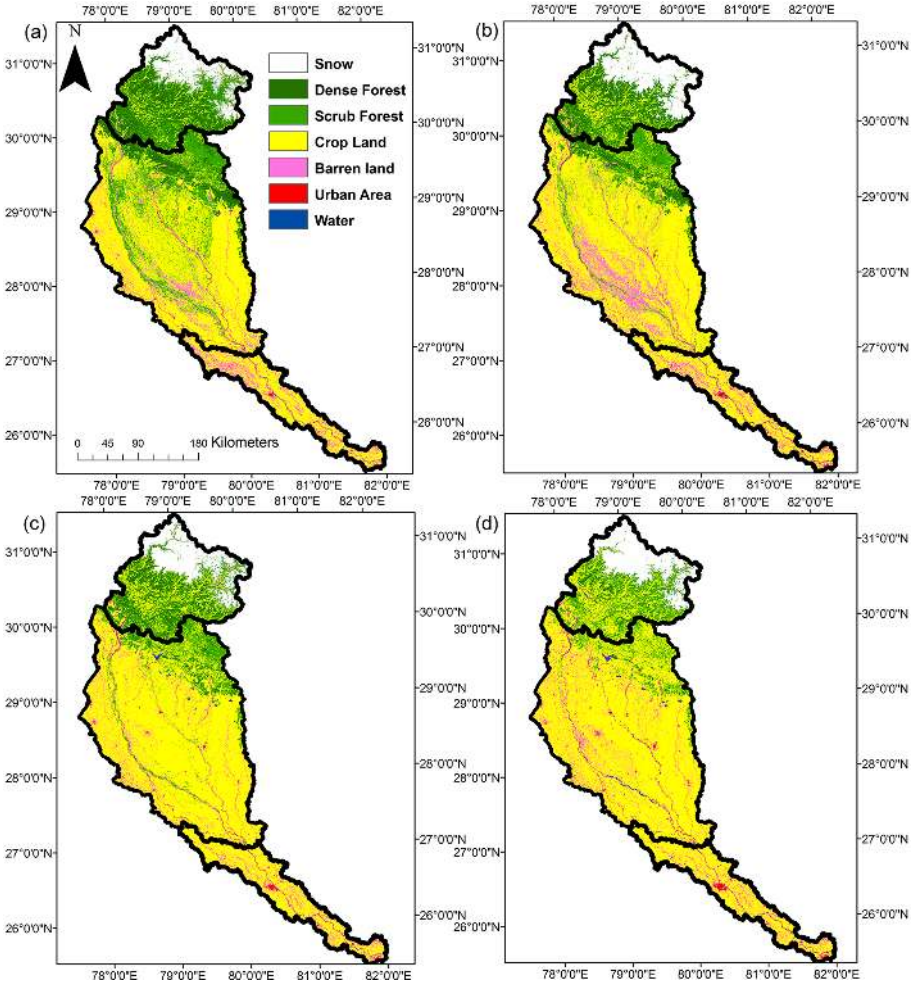

Figure 7. LU maps for **(a)** 1973, **(b)** 1980, **(c)** 2000 and **(d)** 2011.

in all the regions. Results corresponding to ensemble change in mean annual T_{max} and T_{min} from the baseline are shown in Fig. 8, center and bottom panels, respectively. Change in T_{max} and T_{min} can affect the hydrology by changing rain to snow ratio, ET and consequently runoff (Christensen et al., 2004). Therefore, change in T may affect the overall water availability in the basin. On assessing the change in T longitudinally over UGB, it is observed that the downstream region may experience maximum increase in the annual mean T_{max} and T_{min}, thus causing serious implication in this part of the UGB. The downstream region, as mentioned earlier, may suffer from sporadic P along with significant increase in T, resulting in severe water availability problem in this part of the UGB. This condition may prove to be detrimental from agricultural point of view as this area is heavily under cultivation (86 % of total downstream area).

Upon evaluating the emission-scenario-based uncertainty, it is found that there is no significant difference between the two scenarios RCP4.5 and RCP8.5, which indicates that the scenario-based uncertainty will be minimum. Impacts of changes in P and T on streamflow are presented in Sect. 3.3.2.

3.3 Hydrologic responses to land use and climate change

To evaluate the effects of LU and climate change on the hydrology of the study area, three scenarios are considered. The first two scenarios are based on the single factor approach (Li et al., 2009); i.e., one driving factor is changed at an instant keeping the other constant. In the first scenario, climate is considered invariant while LU is varied with time, whereas in the second scenario, LU is considered invariant while climate is varied with time. These two scenarios are constructed to understand how streamflow would respond if only one of the driving forces is changed with time thereby assisting in quantifying the influence of individual factors on streamflow. In reality, both LU and climate change simultaneously with time and the hydrologic response is generated based on their integrated effect which is addressed by the third scenario. Fi-

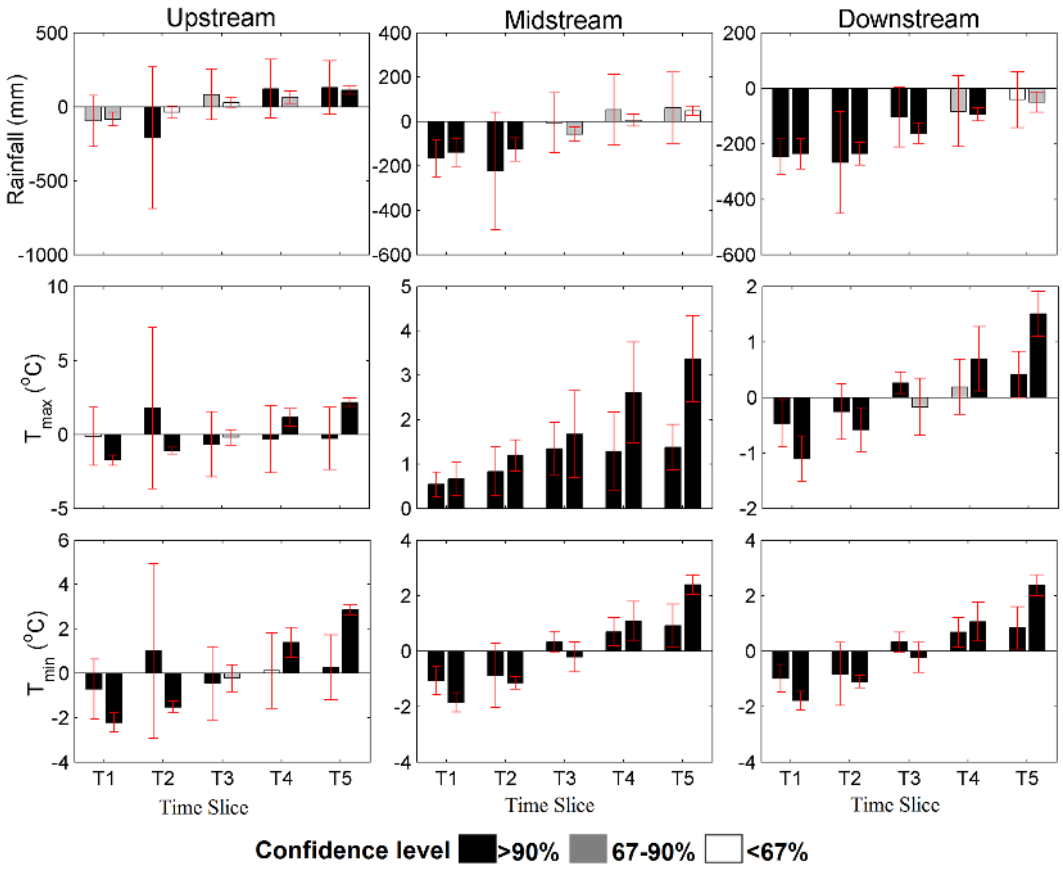

Figure 8. Change in the ensemble mean of rainfall (top panel), T_{max} (center panel) and T_{min} (bottom panel) from the baseline period for RCP4.5 (first bar of a time slice) and RCP8.5 scenarios (second bar of a time slice) at each time slice (T1: 2010–2020, T2: 2021–2040, T3: 2041–2060, T4: 2061–2080 and T5: 2081–2100).

nally, from the integrated response, contributions of LU and climate on the streamflow variability are segregated using results from the other two scenarios. In-depth analysis in the first two scenarios is carried out due to a lack of detailed studies that examine the effects of LU and climate change on streamflow in the UGB.

3.3.1 Impact of land use change

In order to investigate hydrological impacts of LU change, simulations are carried out keeping climate fixed at 1971, while LU is changed progressively from 1971 to 2011. LU in any region changes gradually over a period of time, and therefore starting and ending years may satisfactorily represent the change that has occurred in each LU class. Considering this, LU of the intermittent years can be obtained using rate of change in each LU class between the starting and ending years. It is to be noted that to obtain LU information for 1971 and 1972, rate of change between 1973 and 1980 is considered. LU obtained for each year is then used to drive the VIC model to obtain simulations under LU effect with invariant climate. Although simulations are carried out continuously from 1971 to 2011, for the sake of brevity, results corresponding to the starting year (1971) and the ending year (2011) for all the three regions are presented in Fig. 9.

It can be observed in Fig. 9 that from 1971 to 2011 there is an increase in the magnitude of peak discharge for upstream and midstream regions. This observation is consistent with other studies reported in literature which state that LU change has a pronounced effect on peak flows due to alterations in the infiltration capacity of the surface (Fohrer et al., 2001; Naef et al., 2002; Tollan, 2002; McIntyre et al., 2014). No change in the discharge regime of the downstream region is noticed. LU and topography of the region is observed to have a conspicuous effect on the hydrologic response from the basin which is reflected in the hydrograph patterns for the three regions. The rising limb of the upstream region (Fig. 9a) begins during April while for midstream and downstream (Fig. 9b and c, respectively) it occurs during May–June. The early occurrence of a rising limb in the upstream region can be attributed to the snowmelt-runoff contribution to the streamflow. However, for midstream and downstream regions, a rising limb begins with the onset of monsoon. The recession limb of hydrograph for upstream region falls

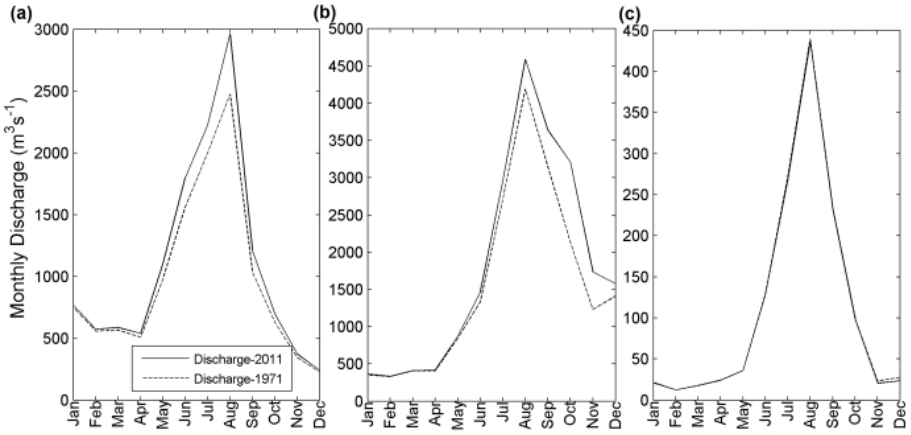

Figure 9. Simulation results for 1971 and 2011 for **(a)** upstream, **(b)** midstream and **(c)** downstream regions.

quickly owing to the steep slope of the region. For the midstream, a sharp drop is observed up to a certain level during October, indicating the termination of direct runoff contribution to streamflow. Following this, the contribution is predominantly through baseflow which in this case is observed to be higher than the baseflow before the monsoon months. The higher baseflow during post-monsoon period could be attributed to slow release of water stored by forests (dense and scrub) in the region aided by low elevation of the terrain in the region. Downstream region, though entirely a flat terrain, is dominated by cropland and urban areas that lack the capacity of holding the water, therefore limiting the contribution of baseflow to streamflow which leads to the observed sharp decline in the recession limb. Furthermore, long-term impacts of LU change are more evident in annual streamflow that is observed to increase by 12, 17 and 1 % from 1971 to 2011 for upstream, midstream and downstream regions, respectively.

Sensitivity of the region to different LU categories is assessed in separate simulations. In this case, simulations considering each LU class are performed and change in streamflow under each category is quantified. To quantify the magnitude of change in streamflow caused by change in LU, the ratio between streamflow and LU is computed. The ratio is referred to as the runoff / LU ratio (RL) in the present study. The RL indicates the effect of 1 % change in any LU category on streamflow and aids in identifying the significance of a particular LU class in determining the hydrologic response. Based on the ratios obtained, streamflow response (to a particular LU category) is classified under three categories: (i) highly sensitive if RL is ≥ 3, which indicates that a change of 1 % in LU category results in the change of hydrologic response by at least 3 times; (ii) moderately sensitive, ($1 \leq \mathrm{RL} < 3$); and (iii) insensitive, ($0 < \mathrm{RL} < 1$). Sign associated with the RL indicates the direction of change.

It can be observed from Table 4 that in the upstream region, RL is maximum for the urban area implying that the hydrologic response in this region is highly sensitive to the changes in urban area. It can be inferred that 1 % change in the urban area results in 4 % increase in the streamflow from the upstream region. The upstream region has a significant portion of area under dense forest that has shown a minor increase in the last decade (2000 to 2011) (Table 3). The simulated streamflow is observed to be moderately sensitive to this increase, though the observed impact is in the opposite direction; i.e., an increase in forest results in a decrease in streamflow. Furthermore, streamflow simulated from the upstream region is moderately sensitive to croplands as well. The midstream region has cropland as the dominant LU type covering 53 % of the area during 1971 and 81 % of the area in 2011; streamflow is observed to be moderately sensitive to it. It is also observed that streamflow is moderately sensitive to urban area in this region. Though the downstream region is predominantly cultivated land (approximately 85 % of the area), hydrologic response is observed to be moderately sensitive to changes in the urban area. High sensitivity of streamflow from the regions to urban area can be attributed to the fact that increase in urban sprawl could reduce the infiltration resulting in the generation of higher surface runoff. In addition to this, it can be observed that hydrologic response to a change in forest area in midstream and downstream regions has a positive sign unlike in the upstream region, where the response has a negative sign. This is due to the fact that midstream and downstream regions are dominated by scrub forest, area under which has decreased over the time period, thereby increasing the streamflow. Thus all three regions of the UGB are observed to be moderately sensitive to a change in cropland area while moderately to highly sensitive to a change in urban area.

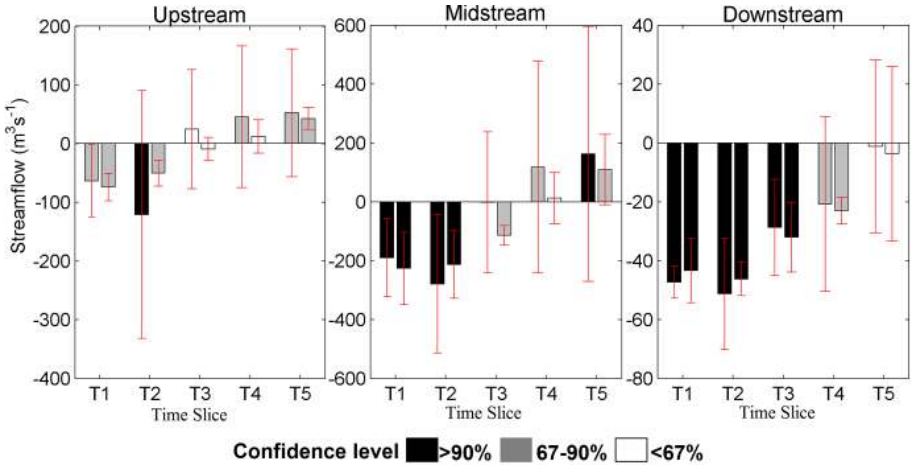

Figure 10. Change in ensemble mean of Q_{clim} from the baseline period for RCP4.5 (first bar of every time slice of all the plots) and RCP8.5 (second bar of every time slice of all the plots) scenarios at each time slice (T1: 2010–2020, T2: 2021–2040, T3: 2041–2060, T4: 2061–2080 and T5: 2081–2100).

Table 4. Runoff / LU ratio for different LU categories for upstream, midstream and downstream regions.

Region	LU classes			
	Crop land	Urban	Forest	Barren
Upstream	2.05	4.02	−1.31	0.91
Midstream	1.49	1.17	0.1	0.97
Downstream	0.63	2.69	0.9	0.93

3.3.2 Impact of climate change

Streamflow observed at Bhimgodha (outlet for upstream region) and Ankinghat (outlet for the midstream region) stations is examined for the presence of a trend using the Mann–Kendall test. It is noticed that the observed streamflow for upstream (1987–2005) and midstream (1977–2005) regions do not show any trend. However, in order to investigate the individual impact of changing climate on hydrology, simulations are carried out keeping LU fixed for 1971 and altering climate continuously for the baseline period (1971–2005) and future emission scenarios (2010–2100). The simulation results obtained are referred to as Q_{clim} hereafter. To quantify the change in streamflow, the VIC model is driven using six downscaled, bias-corrected GCM outputs and the simulation results obtained are compared with the baseline simulation results. Change in ensemble mean annual Q_{clim} for five future time slices from the baseline annual streamflow for the three regions is presented in Fig. 10 with the associated uncertainties shown as error bars.

From the Fig. 10, it can be observed that change in Q_{clim} has patterns similar to that of change in mean annual P (Fig. 8, top panel). Change in Q_{clim} for all the time slices is observed to be moderate to highly significant in most of the cases indicating probable impacts of climate change on hydrologic response of the basin. Uncertainty is observed to increase through the time slices and maximum uncertainty in projection results for all the three regions is observed in T5. Although the two scenarios gave consistent results, to address the issue of scenario-based uncertainty, the mean of the ensemble annual Q_{clim} series of RCP4.5 is compared with the mean of the ensemble annual Q_{clim} series of RCP8.5. The two means are found to be moderately different for the midstream region, indicating the need to consider the two scenarios as separate cases.

Assessment of the monthly variations in the Q_{clim} across future time slices indicated that Q_{clim} may decrease for JAS months for the three regions while it may increase during the months of October, November and December (OND). The variations observed in Q_{clim} during JAS and OND are found to be consistent with that of P. However, this is not true for all the months such as June, where P is observed to decrease in the future while Q_{clim} is observed to increase, which can be attributed to a decrease in T that may reduce evaporation from the region resulting in higher runoff. A similar kind of response of streamflow to $P$and T in a catchment is reported in literature for a different case study by Fu et al. (2007). To further assess the sensitivity of Q_{clim} to changes in P and T and quantify their effect, runoff ratio (RR) is computed using average annual runoff and rainfall for each time slice. Results pertaining to the values of RR are presented in Table 5.

The RR is a simple index that reflects the relationship between P and Q_{clim} by determining the proportion of P that gets converted to Q_{clim} (Zhang et al., 2011). RR is calculated by normalizing the Q_{clim} with P within the same timescale. Analyzing RR over a period of time on the same river basin (under same LU conditions) aids in understanding topographic response and effect of climate on streamflow.

Table 5. Runoff ratio across time slices for upstream, midstream and downstream regions (terms in parentheses indicate the percent change from the baseline values).

Region	Time	Rainfall (mm)		Runoff (mm)		Runoff ratio	
	period	RCP4.5	RCP8.5	RCP4.5	RCP8.5	RCP4.5	RCP8.5
Upstream	Baseline	1294	1294	772	772	0.60	0.60
	T1	1196 ± 172 (−8)	1210 ± 46 (−7)	697 ± 84 (−10)	683 ± 32 (−12)	0.58 (−2)	0.56 (−4)
	T2	1084 ± 480 (−16)	1257 ± 43 (−3)	619 ± 287 (−20)	715 ± 30 (−7)	0.57 (−3)	0.57 (−3)
	T3	1377 ± 171 (+6)	1323 ± 32 (+2)	816 ± 137 (+6)	771 ± 26 (0)	0.59 (−1)	0.58 (−2)
	T4	1416 ± 198 (+9)	1357 ± 42 (+5)	845 ± 163 (+9)	800 ± 38 (+4)	0.60 (0)	0.59 (−1)
	T5	1424 ± 182 (+10)	1405 ± 27 (+9)	854 ± 148 (+11)	842 ± 26 (+9)	0.60 (0)	0.60 (0)
Midstream	Baseline	1009	1009	441	441	0.44	0.44
	T1	844 ± 84 (−16)	871 ± 63 (−14)	323 ± 31 (−27)	328 ± 56 (−25)	0.38 (−12)	0.38 (−4)
	T2	787 ± 265 (−22)	884 ± 53 (−12)	296 ± 115 (−33)	332 ± 52 (−25)	0.38 (−12)	0.38 (−12)
	T3	1003 ± 135 (−1)	952 ± 31 (−6)	413 ± 77 (−6)	378 ± 20 (−14)	0.41 (−3)	0.40 (−4)
	T4	1062 ± 159 (+5)	1016 ± 28 (+1)	462 ± 101 (+5)	427 ± 23 (−3)	0.44 (0)	0.42 (−2)
	T5	1071 ± 160 (+6)	1058 ± 21 (+5)	471 ± 121 (+7)	452 ± 21 (+3)	0.44 (0)	0.43 (−1)
Downstream	Baseline	826	826	192	192	0.23	0.23
	T1	579 ± 63 (−30)	590 ± 55 (−29)	102 ± 13 (−47)	107 ± 19 (−44)	0.18 (−5)	0.18 (−5)
	T2	557 ± 183 (−32)	589 ± 40 (−29)	89 ± 43 (−54)	104 ± 13 (−46)	0.16 (−7)	0.18 (−5)
	T3	721 ± 108 (−13)	663 ± 38 (−20)	141 ± 34 (−27)	127 ± 13 (−34)	0.20 (−3)	0.19 (−4)
	T4	743 ± 128 (−10)	731 ± 23 (−11)	150 ± 46 (−22)	148 ± 7 (−23)	0.20 (−3)	0.20 (−3)
	T5	785 ± 101 (−5)	771 ± 37 (−6)	173 ± 36 (−10)	167 ± 16 (−13)	0.22 (−1)	0.21 (−2)

In the present study, longitudinal variation in RR strikingly depicts the catchment topography from upstream to downstream. RR is observed to be 60 % for the upstream region, 44 % for the midstream region and 23 % for the downstream region during the baseline period. The upstream region is characterized by mountainous terrain and steep slopes; thus, most of the P gets converted to Q_{clim} (high RR), whereas the downstream region has very flat terrain; thus, much of the P gets evaporated or infiltrated into soil and little gets converted to Q_{clim} (low RR). Analysis of RR over the different time slices for a particular region indicates that in general, when P does not change significantly from the baseline period, increase in T results in reduced RR. This is intuitive as increase in T leads to loss of water as evaporation, which reduces Q_{clim} and consequently lessens RR. The RR is observed to increase and approach towards baseline RR with slight increase in P (irrespective of change in T). In such cases, temperature variations are seen to be of less importance. In most of the cases, it is observed that a decrease in P results in a decrease in RR, but in few cases such as T4 and T5 (RCP4.5 and RCP8.5) for a downstream region, P is observed to reduce accompanied by an increase in T. In such a case, one might expect RR to reduce significantly, which is not observed. This anomaly could be attributed to occurrence of short duration dense rainfall events in the region. Reduction in RR is observed in the case when P is observed to increase with no significant change in T. This kind of behavior could be due to a shift in the seasonal pattern of P or due to an increased inter-arrival time between the two P events. In summary, Q_{clim} from the downstream region is observed to

Table 6. Contribution of climate and LU to the streamflow for different time periods.

Region	Streamflow	P1 (1971–1980)	P2 (1981–1990)	P3 (1991–2000)	P4 (2001–2005)
Upstream	Q_{int} ($m^3 s^{-1}$)	775	772	859	823
	Q_{clim} ($m^3 s^{-1}$)	760	741	824	777
	Q_{clim} (%)	98	96	96	94
	Q_{LU} ($m^3 s^{-1}$)	15	31	35	46
	Q_{LU} (%)	2	4	4	6
Midstream	Q_{int} ($m^3 s^{-1}$)	1130	1183	1266	1195
	Q_{clim} ($m^3 s^{-1}$)	1108	1110	1182	1107
	Q_{clim} (%)	98	94	93	93
	Q_{LU} ($m^3 s^{-1}$)	22	73	84	88
	Q_{LU} (%)	2	6	7	7
Downstream	Q_{int} ($m^3 s^{-1}$)	123	103	85	78
	Q_{clim} ($m^3 s^{-1}$)	122	103	85	77
	Q_{clim} (%)	100	100	99	98
	Q_{LU} ($m^3 s^{-1}$)	1	0	1	1
	Q_{LU} (%)	0	0	1	2

be very sensitive to the changes in P, whereas Q_{clim} is sensitive to P up to a certain threshold for the midstream region, beyond which T_{max} also starts playing a role. Owing to the complex topography and climatology of the upstream region, it is difficult to interpret the sensitivity of Q_{clim} to different climate factors.

3.3.3 Integrated impacts of land use and climate change

In a real-world situation, change in LU and climate occurs simultaneously and the impact of both these factors is reflected in the streamflow. To carry out analysis pertaining to this scenario, one needs concurrent information on LU and climate. Under this notion, VIC model is driven for 1971–2005 (baseline period) across the three regions in the UGB. It is to be noted that the process of obtaining projections of future LU conditions in the basin does not come under the purview of the present work. Therefore, integrated impact of LU and climate change on future streamflow could not be assessed. The results obtained from this analysis can be interpreted as the streamflow simulations under simultaneous change in LU and climate conditions (hereafter referred to as Q_{int}). In order to assess decadal variations in streamflow of the UGB, the baseline period is aggregated to four time periods: P1 (1971–1980), P2 (1981–1990), P3 (1991–2000) and P4 (2001–2005), although the VIC model is executed for the entire duration. Results corresponding to Q_{int} for upstream, midstream and downstream regions are presented in Table 6. It is observed that no clear inference about the implication of LU and climate on streamflow can be achieved from the obtained Q_{int} values due to large variability in the streamflow corresponding to the variability in rainfall. Therefore, a further analysis is necessary to isolate the impacts of LU and climate on streamflow response, which is presented in the following sub-section.

3.3.4 Isolating the impacts of land use and climate

In order to segregate the impacts of LU and climate, the proposed approach primarily requires results of Q_{int} (obtained from the Sect. 3.3.3) and Q_{clim} (obtained from the Sect. 3.3.2) over the same time period. Herein Q_{int} and Q_{clim} are comparable based on the fact that the respective simulations are obtained under identical conditions of hydrologic model and climatology. This condition reflects that the only changing subject among the two scenarios is the land use input to the hydrologic model. Therefore, the residue of the two scenarios, $Q_{int} - Q_{clim}$, is considered to be the exclusive contribution of LU to streamflow (hereafter referred to as Q_{LU}). To segregate the contribution of LU and climate from Q_{int}, a linear response of LU and climate to the streamflow is assumed.

In the present case study, simulations of Q_{int} and Q_{clim} are obtained for the time periods P1, P2, P3 and P4 mentioned earlier for upstream, midstream and downstream regions. Q_{int} and Q_{clim} are then used to estimate Q_{LU}. Furthermore, the percentage contributions of LU and climate to Q_{int} are also computed ($Q_{clim(LU)}$ (%) $= \frac{Q_{clim(LU)}}{Q_{int}} \times 100$). Table 6 presents results pertaining to these.

Results from Table 6 suggest that climate is the dominant contributor to streamflow across all the regions. The contribution of LU, on the other hand, is observed to be minimal. Further insight to the influence of LU to streamflow is obtained from the inferences drawn from Sect. 3.3.1. It is observed from the analysis in Sect. 3.3.1 that streamflow is

Table 7. Contribution of LU and climate to streamflow during the T1 (2010–2020) time slice under RCP4.5 and RCP8.5 emission scenarios.

Streamflow	Upstream		Midstream		Downstream	
	RCP4.5	RCP8.5	RCP4.5	RCP8.5	RCP4.5	RCP8.5
Q_{int} ($\text{m}^3\,\text{s}^{-1}$)	800 ± 72	789 ± 28	1008 ± 110	971 ± 138	52 ± 5	56 ± 11
Q_{clim} ($\text{m}^3\,\text{s}^{-1}$)	713 ± 62	703 ± 23	938 ± 132	903 ± 123	51 ± 5	55 ± 11
Q_{clim} (%)	89	89	93	93	98	98
Q_{LU} ($\text{m}^3\,\text{s}^{-1}$)	87 ± 10	86 ± 5	70 ± 23	68 ± 16	1 ± 0	1 ± 0
Q_{LU} (%)	11	11	7	7	2	2

highly sensitive to changes in urban land in upstream and downstream regions, while it is moderately sensitive to urban and cropland areas in the midstream region. The spatial extent of urban area is observed to be much less in upstream and downstream regions (less than 10 %), which could have resulted in a negligible contribution of LU to streamflow. For the midstream region, despite ~ 70 % of the area is under cropland, contribution of LU to streamflow turned out to be less. This could be due to moderate sensitivity of streamflow to the changes in the cropland category. It is well understood that croplands contribute more to the ET than to the streamflow. Contribution of urban area to streamflow is negligible due to its less spatial extent in the midstream region. When Q_{LU} (%) is assessed across the time periods in the three regions, it is observed that there is gradual increase in the contribution of LU to streamflow. This could be attributed to the fact that area under the sensitive LU categories (urban area and cropland) is increasing with time in the regions.

Contribution of LU and climate on the streamflow response is isolated at a monthly scale as well. It is observed that climate is a major contributor to the streamflow across all three regions at a monthly scale as well (see the attached Supplement).

In the present study, the application of proposed methodology of isolating the hydrologic impacts of LU and climate is limited only to the baseline period due to unavailability of future LU information. However, this approach can be applied to the future time periods as well upon obtaining future LU projections along with climate simulations. This is illustrated by conducting the analysis on T1 (2010–2020) wherein Q_{int} is obtained by driving the VIC model under the LU condition of 2011 (assuming that LU may not change significantly during this decade) and climate simulations from six GCMs for the corresponding time period. Results for T1 are presented in Table 7.

From Table 7, it can be observed that the contribution of LU to streamflow from the upstream region has increased (compared to P4). This could be attributed to an increase in area under urban land by 65 % in T1 from P4 in the upstream region. No significant increase is observed in cropland and urban land areas in T1 from P4 for midstream and downstream regions, respectively (2 % increase in cropland in the midstream region and 20 % increase in urban area in the downstream region), which could have resulted in an unvarying contribution of LU to streamflow from P4 (Table 6) to T1 (Table 7) in these regions.

From the analysis, it can be concluded that the proposed approach can be applied over a catchment with a well-calibrated and validated hydrologic model. Future work involves generating LU projections for future time periods, which can be corroborated with climate projections described in Sect. 3.3.2, to isolate the impacts of LU and climate on future streamflow simulations. Although there is the presence of a snow covered region in the basin, segregating the contribution of snowmelt runoff from the total streamflow is not feasible at this stage due to a lack of observed data. This limits the assessment of impact of temperature changes on snowmelt and its consequences on the streamflow.

4 Conclusions

In the present paper a hydrologic modeling-based methodology is presented to isolate the impacts of LU and climate on streamflow in a river basin. To achieve this, three objectives are considered (i) assessing the sensitivity of the streamflow to the changes in LU, (ii) examining the impact of change in climate on the streamflow and (iii) integrated impact of LU and climate change on the streamflow of the UGB. These three objectives are translated to three scenarios and are used to segregate the influence of LU and climate change on the streamflow. Not many studies conducted earlier have considered the combined effect of LU and climate on the hydrology of the basin. The VIC hydrologic model is used to understand the impact of LU and climate change on the streamflow. The VIC model, owing to its comprehensive ability to simulate hydrological processes, has been used widely to perform impact assessment studies. However, being a physically based distributed model, there are concerns associated with the model structure and the number of calibration parameters. Furthermore, due to spatiotemporal variability in the input variables, a parameter set for the initial or reference time period may not be suitable for future periods (Viney et al., 2009). In the present study, these concerns are partially addressed by calibrating and validating the VIC model over upstream, midstream and downstream regions of the UGB.

LU change analysis of the study region indicated an increase in the areas of crop and urban land categories to which streamflow is observed to be moderately to highly sensitive. From the climate change analysis, it is observed that rainfall may decrease during the monsoon months and increase during the winter months which may result in a shift in seasonal rainfall pattern. Annual means of T_{max} and T_{min} are observed to increase in the future. Streamflow is observed to reproduce the variations in rainfall. All the changes in rainfall, T_{max} and T_{min} pertaining to climate change scenario are found to be statistically significant from the baseline period, indicating that deviation in their magnitudes is likely to cause serious impacts on the hydrologic response. It may be noted that the meteorological variables from only six GCMs are used for the analysis, which is a limitation of the study. There is a need to consider more GCMs to address the issue of model and scenario-based uncertainty more comprehensively.

The integrated effect of LU and climate change on streamflow is observed to be more prominent in the study area. From the analysis of isolating the individual impacts of LU and climate from their integrative effects on streamflow, it is observed that climate contributes more to the simulated streamflow ($> 90\,\%$). In contrast, LU did not contribute significantly to the simulated streamflow that could be attributed to less spatial extent of sensitive LU categories in the region.

The proposed approach is generic and applicable to any river basin to isolate the relative impacts of LU and climate change on streamflow. However, the approach is based on the assumption of linear response of LU and climate to the streamflow. The case study analysis indicates that the change in climate may become a major concern in the UGB for water resources management.

The Supplement related to this article is available online at doi:10.5194/hess-19-3633-2015-supplement.

Acknowledgements. The authors would like to thank Thomas Kjeldsen (manuscript handling editor), Ge Sun, Young-Oh Kim and the anonymous referees for providing very useful comments on the manuscript. The work is carried out as part of the MoES-NERC Changing Water Cycle (South Asia) project: hydro-meteorological feedbacks and changes in water storage and fluxes in Northern India (grant no. MoES/NERC/16/02/10 PC-II). Authors acknowledge the support of the Indian Meteorological Department (IMD) and the Indian Institute of Tropical Meteorology (IITM) for providing the data.

Edited by: T. Kjeldsen

References

Arnell, N. W.: Uncertainty in the relationship between climate forcing and hydrological response in UK catchments, Hydrol. Earth Syst. Sci., 15, 897–912, doi:10.5194/hess-15-897-2011, 2011.

Arora, V. K. and Boer, G. J.: Effects of simulated climate change on the hydrology of major river basins, J. Geophys. Res.-Atmos., 106, 3335–3348, doi:10.1029/2000JD900620, 2001.

Beyene, T., Lettenmaier, D. P., and Kabat, P.: Hydrologic impacts of climate change on the Nile River Basin: implications of the 2007 IPCC scenarios, Climatic Change, 100, 433–461, doi:10.1007/s10584-009-9693-0, 2010.

Christensen, N. S. and Lettenmaier, D. P.: A multimodel ensemble approach to assessment of climate change impacts on the hydrology and water resources of the Colorado River Basin, Hydrol. Earth Syst. Sci., 11, 1417–1434, doi:10.5194/hess-11-1417-2007, 2007.

Christensen, N. S., Wood, A. W., Voisin, N., Lettenmaier, D. P., and Palmer, R. N.: The effects of climate change on the hydrology and water resources of the Colorado River basin, Climatic Change, 62, 337–363, doi:10.1023/B:CLIM.0000013684.13621.1f, 2004.

Cuo, L., Zhang, Y., Gao, Y., Hao, Z., and Cairang, L.: The impacts of climate change and land cover/use transition on the hydrology in the upper Yellow River Basin, China, J. Hydrol., 502, 37–52, doi:10.1016/j.jhydrol.2013.08.003, 2013.

Ekström, M., Jones, P. D., Fowler, H. J., Lenderink, G., Buishand, T. A., and Conway, D.: Regional climate model data used within the SWURVE project – 1: projected changes in seasonal patterns and estimation of PET, Hydrol. Earth Syst. Sci., 11, 1069–1083, doi:10.5194/hess-11-1069-2007, 2007.

Fohrer, N., Haverkamp, S., Eckhardt, K., and Frede, H. G.: Hydrologic response to land use changes on the catchment scale, Phys. Chem. Earth B, 26, 577–582, doi:10.1016/S1464-1909(01)00052-1, 2001.

Fu, G., Charles, S. P., and Chiew, F. H. S.: A two-parameter climate elasticity of streamflow index to assess climate change effects on annual streamflow, Water Resour. Res., 43, W11419, doi:10.1029/2007wr005890, 2007.

Ghosh, S. and Mujumdar, P. P.: Climate change impact assessment: Uncertainty modeling with imprecise probability, J. Geophys. Res.-Atmos., 114, D18113, doi:10.1029/2008jd011648, 2009.

Giorgi, F. and Mearns, L. O.: Calculation of average, uncertainty range, and reliability of regional climate changes from AOGCM simulations via the "reliability ensemble averaging" (REA) method, J. Climate, 15, 1141–1158, doi:10.1175/1520-0442(2002)015<1141:coaura>2.0.co;2, 2002.

Gleick, P. H.: Methods for evaluating the regional hydrologic impacts of global climatic changes, J. Hydrol., 88, 97–116, doi:10.1016/0022-1694(86)90199-X, 1986.

Guo, H., Hu, Q., and Jiang, T.: Annual and seasonal streamflow responses to climate and land-cover changes in the Poyang Lake basin, China, J. Hydrol., 335, 106–122, doi:10.1016/j.jhydrol.2008.03.020, 2008.

Hamlet, A. F. and Lettenmaier, D. P.: Effects of climate change on hydrology and water resources in the Columbia River basin, J. Am. Water Resour. Assoc., 35, 1597–1623, doi:10.1111/j.1752-1688.1999.tb04240.x, 1999.

Islam, S. A., Bari, M. A., and Anwar, A. H. M. F.: Hydrologic impact of climate change on Murray–Hotham catchment of West-

ern Australia: a projection of rainfall–runoff for future water resources planning, Hydrol. Earth Syst. Sci., 18, 3591–3614, doi:10.5194/hess-18-3591-2014, 2014.

Kendall, M. G.: A new measure of rank correlation, Biometrika, 30, 81–93, 1938.

Li, Z., Liu, W.-Z., Zhang, X.-C., and Zheng, F.-L.: Impacts of land use change and climate variability on hydrology in an agricultural catchment on the Loess Plateau of China, J. Hydrol., 377, 35–42, doi:10.1016/j.jhydrol.2009.08.007, 2009.

Liang, X., Lettenmaier, D. P., Wood, E. F., and Burges, S. J.: A simple hydrologically based model of land-surface water and energy fluxes for general-circulation models, J. Geophys. Res.-Atmos., 99, 14415–14428, doi:10.1029/94jd00483, 1994.

Lohmann, D., Raschke, E., Nijssen, B., and Lettenmaier, D. P.: Regional scale hydrology: I. Formulation of the VIC-2L model coupled to a routing model, Hydrolog. Sci. J., 43, 131–141, doi:10.1080/02626669809492107, 1998.

Lørup, J. K., Refsgaard, J. C., and Mazvimavi, D.: Assessing the effect of land use change on catchment runoff by combined use of statistical tests and hydrological modelling: case studies from Zimbabwe, J. Hydrol., 205, 147–163, doi:10.1016/S0168-1176(97)00311-9, 1998.

Mango, L. M., Melesse, A. M., McClain, M. E., Gann, D., and Setegn, S. G.: Land use and climate change impacts on the hydrology of the upper Mara River Basin, Kenya: results of a modeling study to support better resource management, Hydrol. Earth Syst. Sci., 15, 2245–2258, doi:10.5194/hess-15-2245-2011, 2011.

Mann, H. B.: Nonparametric tests against trend, Econometrica, 13, 245–259, doi:10.2307/1907187, 1945.

Maurer, E. P.: Uncertainty in hydrologic impacts of climate change in the Sierra Nevada, California, under two emissions scenarios, Climatic Change, 82, 309–325, doi:10.1007/s10584-006-9180-9, 2007.

Maurer, E. P. and Hidalgo, H. G.: Utility of daily vs. monthly large-scale climate data: an intercomparison of two statistical downscaling methods, Hydrol. Earth Syst. Sci., 12, 551–563, doi:10.5194/hess-12-551-2008, 2008.

McIntyre, N., Ballard, C., Bruen, M., Bulygina, N., Buytaert, W., Cluckie, I., Dunn, S., Ehret, U., Ewen, J., Gelfan, A., Hess, T., Hughes, D., Jackson, B., Kjeldson, T., Merz, R., Park, J., O'Connell, E., O'Donnell, G., Oudin, L., Todini, E, Wagener, T., and Wheater, H.: Modelling the hydrological impacts of rural land use change, Hydrol. Res., 45, 737–754, doi:10.2166/nh.2013.145, 2014.

Naef, F., Scherrer, S., and Weiler, M.: A process based assessment of the potential to reduce flood runoff by land use change, J. Hydrol., 267, 74–79, doi:10.1016/S0022-1694(02)00141-5, 2002.

Nijssen, B., O'Donnell, G. M., Hamlet, A. F., and Lettenmaier, D. P.: Hydrologic sensitivity of global rivers to climate change, Climatic Change, 50, 143–175, doi:10.1023/a:1010616428763, 2001.

Nohara, D., Kitoh, A., Hosaka, M., and Oki, T.: Impact of climate change on river discharge projected by multimodel ensemble, J. Hydrometeorol., 7, 1076–1089, doi:10.1175/JHM531.1, 2006.

Oki, T. and Kanae, S.: Global hydrological cycles and world water resources, Science, 313, 1068–1072, doi:10.1126/science.1128845, 2006.

Ott, B. and Uhlenbrook, S.: Quantifying the impact of land-use changes at the event and seasonal time scale using a process-oriented catchment model, Hydrol. Earth Syst. Sci., 8, 62–78, doi:10.5194/hess-8-62-2004, 2004.

Rajeevan, M., Bhate, J., Kale, J. A., and Lal, B.: High resolution daily gridded rainfall data for the Indian region: Analysis of break and active monsoon spells, Curr. Sci. India, 91, 296–306, 2006.

Refsgaard, J. C. and Knudsen, J.: Operational validation and intercomparison of different types of hydrological models, Water Resour. Res., 32, 2189–2202, doi:10.1029/96wr00896, 1996.

Renner, M., Seppelt, R., and Bernhofer, C.: Evaluation of water-energy balance frameworks to predict the sensitivity of streamflow to climate change, Hydrol. Earth Syst. Sci., 16, 1419–1433, doi:10.5194/hess-16-1419-2012, 2012.

Renner, M., Brust, K., Schwaerzel, K., Volk, M., and Bernhofer, C.: Separating the eects of changes in land cover and climate: a hydro-meteorological analysis of the past 60 yr in Saxony, Germany, Hydrol. Earth Syst. Sci., 18, 389–405, doi:10.5194/hess-18-389-2014, 2014.

Rientjes, T. H. M., Haile, A. T., Kebede, E., Mannaerts, C. M. M., Habib, E., and Steenhuis, T. S.: Changes in land cover, rainfall and stream flow in Upper GilgelAbbay catchment, Blue Nile basin-Ethiopia, Hydrol. Earth Syst. Sci., 15, 1979–1989, doi:10.5194/hess-15-1979-2011, 2011.

Rose, S. and Peters, N. E.: Effects of urbanization on streamflow in the Atlanta area (Georgia, USA): a comparative hydrological approach, Hydrol. Process., 15, 1441–1457, doi:10.1002/hyp.218, 2001.

Scanlon, B. R., Jolly, I., Sophocleous, M., and Zhang, L.: Global impacts of conversions from natural to agricultural ecosystems on water resources: Quantity versus quality, Water Resour. Res., 43, W03437, doi:10.1029/2006wr005486, 2007.

Sheffield, J., Goteti, G., and Wood, E. F.: Development of a 50-year high-resolution global dataset of meteorological forcings for land surface modeling, J. Climate, 19, 3088–3111, doi:10.1175/JCLI3790.1, 2006.

Singh, D., Horton, D. E., Tsiang, M., Haugen, M., Ashfaq, M., Mei, R., Rastogi, D., Johnson, N. C., Charland, A., Rajaratnam, B., and Diffenbaugh, N. S.: Severe precipitation in northern india in june 2013: causes, historical context, and changes in probability, B. Am. Meteorol. Soc., 95, S58–S61, 2014.

Tollan, A.: Land-use change and floods: what do we need most, research or management?, Water Sci. Technol., 45, 183–190, 2002.

Tsarouchi, G., Mijic, A., Mould, S., and Buytaert, W.: Historical and future land-cover changes in the Upper Ganges basin of India, Int. J. Remote Sens., 35, 3150–3176, doi:10.1080/01431161.2014.903352, 2014.

Viney, N. R., Bormann, H., Breuer, L., Bronstert, A., Croke, B. F. W., Frede, H., Gräff, T., Hubrechts, L., Huisman, J. A., Jakeman, A. J., Kite, G. W., Lanini, J., Leavesley, G., Lettenmaier, D. P., Lindström, G., Seibert, J., Sivapalan, M., and Willems, P.: Assessing the impact of land use change on hydrology by ensemble modelling (LUCHEM) II: Ensemble combinations and predictions, Adv. Water Resour., 32, 147–158, doi:10.1016/j.advwatres.2008.05.006, 2009.

Vörösmarty, C. J., Green, P., Salisbury, J., and Lammers, R. B.: Global water resources: Vulnerability from cli-

mate change and population growth, Science, 289, 284–288, doi:10.1126/science.289.5477.284, 2000.

Wada, Y., van Beek, L. P. H., and Bierkens, M. F. P.: Modelling global water stress of the recent past: on the relative importance of trends in water demand and climate variability, Hydrol. Earth Syst. Sci., 15, 3785–3808, doi:10.5194/hess-15-3785-2011, 2011.

Wagner, P. D., Kumar, S., and Schneider, K.: An assessment of land use change impacts on the water resources of the Mula and Mutha Rivers catchment upstream of Pune, India, Hydrol. Earth Syst. Sci., 17, 2233–2246, doi:10.5194/hess-17-2233-2013, 2013.

Wang, D. and Hejazi, M.: Quantifying the relative contribution of the climate and direct human impacts on mean annual streamflow in the contiguous United States, Water Resour. Res., 47, W00J12, doi:10.1029/2010WR010283, 2011.

Wang, G. Q., Zhang, J. Y., Jin, J. L., Pagano, T. C., Calow, R., Bao, Z. X., Liu, C. S., Liu, Y. L., and Yan, X. L.: Assessing water resources in China using PRECIS projections and a VIC model, Hydrol. Earth Syst. Sci., 16, 231–240, doi:10.5194/hess-16-231-2012, 2012.

Wang, S., Kang, S., Zhang, L., and Li, F.: Modelling hydrological response to different land-use and climate change scenarios in the Zamu River basin of northwest China, Hydrol. Process., 22, 2502–2510, doi:10.1002/hyp.6846, 2008.

Wang, S., Zhang, Z., McVicar, T. R., Guo, J., Tang, Y., and Yao, A.: Isolating the impacts of climate change and land use change on decadal streamflow variation: Assessing three complementary approaches, J. Hydrol., 507, 63–74, doi:10.1016/j.jhydrol.2013.10.018, 2013.

Wood, A. W., Maurer, E. P., Kumar, A., and Lettenmaier, D. P.: Long-range experimental hydrologic forecasting for the eastern United States, J. Geophys. Res.-Atmos., 107, ACL 6-1–ACL 6-15, doi:10.1029/2001jd000659, 2002.

Zhang, X., Zhang, L., Zhao, J., Rustomji, P., and Hairsine, P.: Responses of streamflow to changes in climate and land use/cover in the Loess Plateau, China, Water Resour. Res., 44, W00A07, doi:10.1029/2007WR006711, 2008.

Zhang, Y., Guan, D., Jin, C., Wang, A., Wu, J., and Yuan, F.: Analysis of impacts of climate variability and human activity on streamflow for a river basin in northeast China, J. Hydrol., 410, 239–247, 2011.